High Energy Telescopes in the Advanced Detector Network

Mentors: Leo Singer and Larry Price

David R. Miller[1]

[1] *Carleton College, One North College Street, Northfield, Minnesota 55057*

(Dated: September 27, 2012)

The detection of gravitational waves from compact binary coalescence mergers are likely when the Advanced LIGO/Virgo detector network goes online as early as 2015. To maximize the science returns and confirm gravitational wave detection, an electromagnetic counterpart must be detected. I examine the ability of the *Swift*, *Fermi*, and *SVOM* telescopes to detect short gamma-ray bursts in coincidence with gravitational wave signals.

I. INTRODUCTION

When a mass accelerates, it creates a ripple through the fabric of space-time. These ripples are known as gravitational waves (GWs). The theory of general relativity predicts the existence of GWs, but they have never been directly observed, only indirectly via electromagnetic (EM) radiation. As ground-based gravitational-wave detectors enter the advanced detector era, the most promising source for detecting GWs is coalescing neutron-star (NS) and black-hole (BH) binary systems with an expected combined event rate of 50 per year for the Advanced LIGO/Virgo detector network (hereafter ALIGO/Virgo) [1]. The coalescence of two compact objects can be split into three stages. First, a relatively long inspiral phase in which the compact objects emit GWs causing their orbits to shrink. Next, a relatively short merger phase when the two objects collide into each other. Finally, a ringdown phase in which the single newly-formed compact object, typically a black hole, stabilizes into a stationary state [2]. The end of the inspiral phase is expected to emit GW transients detectable by ALIGO/Virgo, and seconds after merger is expected to emit EM transients, namely short gamma ray bursts (SGRBs), detectable by high-energy telescopes such as the *Fermi* and *Swift* telescopes ([1],[3]). Detecting the presence of SGRBs increases parameter estimation by reducing parameter degeneracies and allows for a measurement of the merger redshift [3].

II. SHORT GAMMA-RAY BURSTS

NS-NS and NS-BH binary systems are expected progenitors of SGRBs. After the merger, an accretion disk (blue in Figure 1) forms around the newly formed object, creating collimated relativistic jets. The jets propagate outward into the surrounding medium (pink in Figure 1), producing a prompt SGRB. As the jet interacts with the surrounding medium, it engenders EM radiation across numerous energy bands, called an afterglow. This paper focuses on the X-ray afterglow, which is observable seconds after the prompt SGRB and can last for hours. [3]

SGRBs are characterized by two angles: the jet half-opening angle θ_j, which is the angle between the center and edge of the collimated jet, and the observer angle θ_o, which is the angle between the observer and the center of the collimated jet. Typically, SGRBs are detected only if the observer angle is within the half-opening angle of the jet, for which an observer is expected to detect the GW signal seconds before the EM signal from the prompt SGRB [2]. There have been only four measured jet half-opening angles: $\sim 6°$, $\sim 6°$, $\sim 7°$, and $\sim 22°$ [4]. Other parameters include the total energy released in both jets, E, which typically ranges from 10^{48} – 10^{58} ergs [5], and the circumburst particle density, n, which typically ranges from 10^{-5} – 1 cm^{-3} [5]. Figure 2 depicts these parameters.

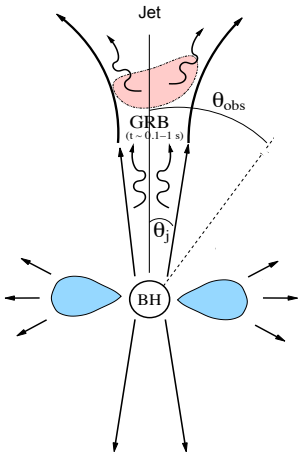

FIG. 1: Illustration of the formation of a prompt SGRB. The accretion disks (blue) around the newly formed compact object (BH) cause collimated relativistic jets to form, producing a SGRB. The interaction of the jets with the surrounding medium (pink) engenders an afterglow across EM bands ranging from X-ray to radio [3]. Note: Image adopted from Metzger and Berger [3].

There are two approaches to detect SGRBs in coincidence with GW signals. One approach is to detect a SGRB with high energy telescopes and then check GW data for a signal. The second approach is to detect a GW signal and then search for EM counterparts with high energy telescopes. The beneficial aspect of the former ap-

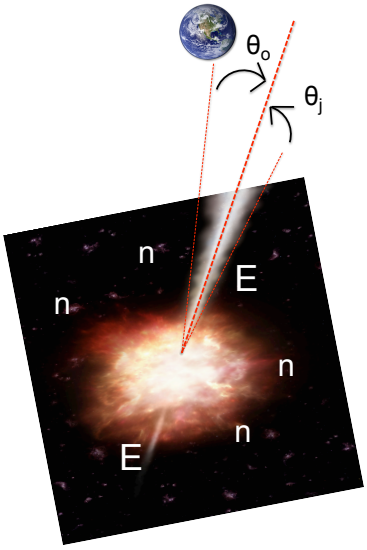

FIG. 2: Depiction of the parameters of a SGRB. θ_o is the observer angle, θ_j is the jet half-opening angle, E is the total energy released in both jets, and n is the circumburst particle density.

proach is that SGRBs have a temporal coincidence with GW chirp signals, however, no SGRB with an identified redshift has ever been observed within the ALIGO/Virgo sensitivity range for NS-NS binary systems and only two within the NS-BH sensitivity range [3]. The beneficial aspect of the latter approach is that GW detectors are all-sky instruments, while telescopes are limited to detecting sources within their field of views. However, the source localization error region for ALIGO/Virgo is large because the network consists of only a few detectors. In this paper, I will focus on the latter approach, using GW signals to search for SGRBs. I am consequently assuming that GW chirp signals detected by ALIGO/Virgo are localized in real time. This makes it possible to direct high energy telescopes at GW signal localization error regions within minutes after the initial GW signal, allowing high energy telescopes to search the localization error region for the X-ray afterglow of the SGRB. The predicted error regions for ALIGO/Virgo are as low as 20 square degrees when ALIGO/Virgo reaches its designed sensitivity [6]. However, during the initial stages, or perhaps for weak signals with low SNR (signal to noise ratio), the error region could be as high as 100 square degrees [7].

ALIGO/Virgo expect to detect 40 NS-NS and 10 NS-BH merger events per year, assuming a horizon distance of 445 Mpc for NS-NS mergers and 927 Mpc for NS-BH mergers, and a mass of 1.4 $M_\odot$ for a NS and 10 $M_\odot$ for a BH [8]. The horizon distance is the distance to which an optimally located and oriented system can be detected with a SNR threshold of 8, while the range of an object is the distance to which a system with sky location and orientation averaged over the search volume can be detected for a SNR threshold of 8. The range for ALIGO/Virgo is ∼200 Mpc for NS-NS systems and ∼410 Mpc for NS-BH systems [8]. Scaling the expected volumetric SGRB rate to the corresponding range yields an event rate of 0.3 and 3 SGRBs per year in coincidence with NS-NS and NS-BH mergers, respectively ([3], [9]). The beaming of the collimated jets causes the detection of prompt SGRBs to be significantly fewer than their GW counterparts.

III. METHODS

The goal of my project was to determine the best telescope at detecting X-ray afterglows of prompt SGRBs. My figure of merit for the best telescope is the amount of time that a telescope can wait to point at a SGRB-producing source and still make a detection of the X-ray afterglow. The telescope that can can afford the most time is consequently the best telescope for detecting X-ray afterglows of SGRBs. To investigate, I simulated a prompt SGRB and its X-ray afterglow, and modeled the detection of the X-ray afterglow by various telescopes. In order to simulate a SGRB and its X-ray afterglow, I defined the parameters of a *typical* SGRB to be those seen in Table I; I chose the *typical* values to be approximately the average of the minimum and maximum range.

TABLE I: Parameters of SGRB

Parameter	Minimum	Maximum	***Typical***
E	10^{48} ergs	10^{50} ergs	$\mathbf{10^{49}}$ **ergs**
n	10^{-5} cm^{-3}	1 cm^{-3}	$\mathbf{10^{-3}}$ **cm**$^{-3}$
θ_{jet}	6°	22°	**11°**
θ_{obs}	0°	$\sim \theta_{jet}$	**5.5°**

To simulate a SGRB and its X-ray afterglow, I used the code *Boxfit* developed by van Eerten et al. [10], which uses relativistic adaptive mesh refinement hydrodynamics to compute the evolution of the collimated jets that produce the SGRB and its X-ray afterglow. Boxfit produces the energy flux density of a SGRB as it evolves in time at a single photon frequency given various input parameters. I performed simulations for the specified *typical* parameters in Table I over numerous photon frequencies in the X-ray range. In my simulations, I assumed a synchrotron slope of p=2.5, a magnetic field energy fraction of ϵ_B=0.01, an accelerated particle energy density fraction of ϵ_E=0.1, an accelerated particle number density fraction of ξ_N=1.0, and a redshift of z=0.05.

I performed each simulation for a 20 minute period following the prompt SGRB. To determine the number of photons a telescope detects for a starting observation time after the prompt SGRB, t_{obs}, and an ending observation time of 20 minutes after the initial prompt SGRB, I related the total number of photons detected, N, to en-

ergy flux density, $S(t, E_{phot})$:

$$N = \int_{t_{obs}}^{20\ min} \int_{E_1}^{E_2} \frac{S(t, E_{phot}) \cdot A_{eff}(E_{phot})}{E_{phot}} \cdot dE_{phot} \cdot dt \tag{3.1}$$

where E_2 and E_1 are the maximum and minimum energy range of the telescope respectively, A_{eff} is the effective area of the telescope, E_{phot} is the photon energy, and t is time. Hence, l determined N for a telescope using the simulated energy flux density within the telescope's sensitive energy range and its effective area.

I assumed a telescope made a detection when the telescope's SNR equaled 5 or greater. Following Poisson statistics, I defined the SNR, σ, as:

$$\sigma = \frac{N}{\sqrt{N + N_{BG}^2}} \tag{3.2}$$

where N is the number of detected photons and N_{BG} is the diffuse background noise as determined by Gruber [11]. The numerator is thus the number of photons detected by the telescope from the signal, and the denominator is the number of photons detected by the telescope as noise. Note that if N_{BG} is negligible, N=25 photons corresponds to a detection.

IV. TELESCOPES

I compared the performance of gamma-ray and X-ray telescopes onboard the *Swift*, *Fermi*, and *SVOM* telescopes for the range of parameters previously specified. The characteristics of the telescopes are outlined in Table II.

A. *Swift*

The *Swift* telescope, launched in 2004, uses the Burst Alert Telescope (BAT) to detect prompt SGRBs and initially localize the source, and then slews the X-ray Telescope (XRT) to search for X-ray afterglows. BAT has a sensitive energy range primarily between 15–150 keV that can extend up to 500 keV [12], which is technically in the hard X-ray spectrum. BAT has a ∼4600 square degree FOV and effective area of ∼1,400 cm^2 at 60 keV [12]. BAT's primary objective is detecting prompt SGRBs; it performs an all-sky hard X-ray survey and monitors for hard X-ray transients to search for bursts [13]. XRT is sensitive in the energy range of 0.2 - 10 keV with a ∼0.16 square degree FOV and effective area of 110 cm^2 at 1.5 keV [12].

B. Fermi

The *Fermi* telescope, launched in 2008, uses the Gamma-ray Burst Monitor (GBM) to detect both prompt SGRBs and their X-ray afterglows. The GBM covers the energy range from ∼8 keV to ∼1 MeV [14], and has a monstrous FOV of ∼31,000 square degrees but comparatively small effective area of ∼100 cm^2 at 100 keV [14].

C. SVOM

The *SVOM* telescope, expected to launch in 2017, will use ECLAIR for detecting prompt SGRBs and initially localizing sources. The Microchannel X-ray Telescope (MXT) will then inspect the localization region for X-ray afterglows. ECLAIR has a sensitive energy range between 4–250 keV and is expected to be more sensitive to soft gamma-ray bursts (∼4-20 keV) than BAT and GBM [15]. ECLAIR will have a ∼6,500 square degree FOV and effective area of ∼1,000 cm^2 at 60 keV [15]. MXT will have a ∼0.2 square degree FOV, covering the entire localization error region of ECLAIR, and a 50 cm^2 effective area at 1 keV [16].

V. RESULTS AND DISCUSSION

Figure 3 shows the number flux density in time of the simulated *typical* SGRB for photon energies ranging from 0.2 keV to 1000 keV. Labels to the right of the plot indicate the corresponding photon energies and sensitive energy ranges of XRT, BAT, GBM, ECLAIR and MXT. The number flux density increases as photon energy decreases, indicating there are more photons to detect at low energies ($\gtrsim$10 keV) than at high energies ($\lesssim$100 keV). Thus, XRT and MXT are quality candidates for detecting X-ray afterglows; however, the effective area and field of vision of the telescope also play a crucial role in the actual number of photons that a telescope detects. Figures 4 and 5 compare the actual number of photons the telescopes would detect for a *typical* SGRB as determined by Equation 3.1. The telescope starting observation time, t_{obs}, is indicated as "Time after prompt SGRB" and the ending observation time is 20 minutes.

Figure 4 shows the number of photons detected by the telescopes for a source distance of d=200 Mpc, the range of ALIGO/Virgo for NS-NS binary systems. In order for a telescope to make a detection, it must detect more photons than the dotted black line indicating an SNR threshold of 5 (the brown dotted line incorporates an approximated average of the background noise, while the black line assumes the background noise is negligible). The plot illustrates that for d=200 Mpc, ECLAIR, XRT, and BAT would make a detection of the X-ray afterglow while MXT and GBM would not. To make a detection for an ending observation time 20 minutes after the prompt SGRB, ECLAIR must start its observation within 750 seconds, XRT within 86 seconds, and BAT within 55 seconds after the initial prompt SGRB. ECLAIR performs significantly better than the other telescopes because it

TABLE II: Telescope Overview

Telescope	Energy (keV)	FOV (degrees^2)	Effective Area (cm^2)	Detection Purpose
BAT (Swift)	15–150	2,600	1,400 at 60 keV	Prompt SGRB
XRT (Swift)	0.2–10	0.16	110 at 1.5 keV	X-ray afterglow
GBM (Fermi)	8–1000	31,000	100 at 100 keV	Prompt SGRB / X-ray afterglow
ECLAIR (SVOM)	4–250	6,500	1,000 at 60 keV	Prompt SGRB
MXT (SVOM)	0.3–6	0.2	50 at 1 keV	X-ray afterglow

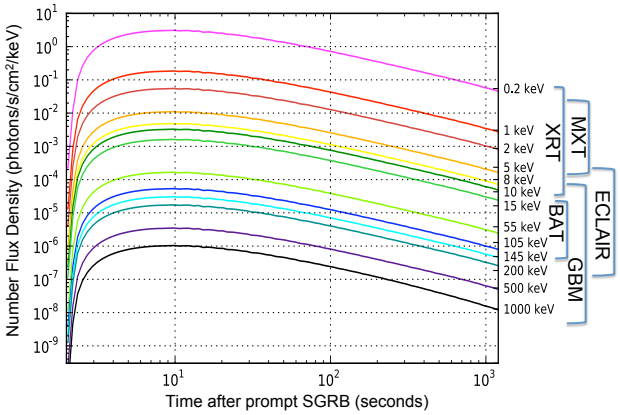

FIG. 3: Plot of the number flux density for various photon frequencies ranging from 0.2 keV to 1000 keV. Each line corresponds to the number flux density for the photon energy on the right. The sensitive energy ranges for the *Swift*, *Fermi*, and *SVOM* telescopes are outlined on the right.

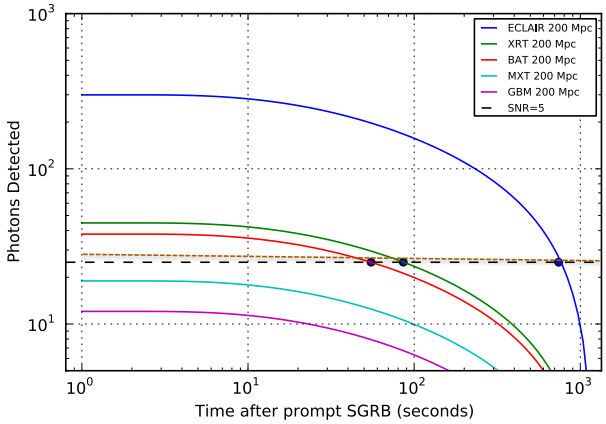

FIG. 4: Photons detected by XRT, BAT, GBM, ECLAIR, and MXT for d=200 Mpc and ending observation time of 20 minutes after the initial prompt SGRB. As indicated by the small dots, ECLAIR must start its observation within 750 seconds after the prompt SGRB, XRT within 86 seconds, and BAT within 55 seconds; MXT and GBM would not make a detection regardless of when they start observing. The black dotted line is the SNR threshold of 5 assuming the background is negligible, while the brown dotted line incorporates an approximated average of the background noise for all of the telescopes.

has a relatively large effective area and is sensitive to photon energies down to 4 keV. It is surprising that BAT performs almost as well as XRT, since the *Swift* telescope typically uses BAT to detect prompt SGRB and then employs XRT to detect X-ray afterglows.

Figure 5 shows the number of photons detected by the telescopes for a source distance of d=20 Mpc. At such a small astronomical distance, all of the telescopes should observe the X-ray afterglow. This is indeed what the plot illustrates: ECLAIR, XRT, and BAT can wait to the last second of the 20 minute observation time and still detect the X-ray afterglow, while MXT must start its observation within 1115 seconds following the prompt SGRB, and GBM within 1040 seconds. Again, BAT surprisingly performs almost as well XRT.

To compare the performance of BAT and XRT more closely, Figure 6 shows the number of photons detected by BAT and XRT for source distances of d=20, 80, 140, and 200 Mpc. For d=200 Mpc, XRT only has an extra 31 seconds before it must start its observation (86 s / 55 s); for d= 140 Mpc, XRT has an extra 64 seconds (304 s / 240 s); and for d=80 Mpc, XRT has an extra 60 seconds (740 s / 680 s). Since BAT is typically used solely for detecting prompt SGRBs and initially localizing the source instead of X-ray afterglows, it is surprising the BAT performs comparable to XRT at detecting X-ray afterglows. This suggests that BAT may be more versatile than expected, as it can detect prompt SGRBs at its peak energy sensitivity around 150 keV as well as X-ray afterglows at its minimum energy sensitivity around 15 keV. Unfortunately, there have been no observed SGRBs with identified redshifts within d=200 Mpc for which BAT data can be examined to directly verify the findings of my simulations. However, BAT detections of other kinds of bursts have occurred within d=200 Mpc and could reveal more details on whether BAT truly could detect X-ray afterglows to similar sensitivities of XRT for source distances within 200 Mpc. Examining gamma-ray bursts detected by BAT within a few hundred Mpc and performing more and longer duration simulations over the entire parameter space of SGRBs will help determine BAT's true potential for detecting X-ray afterglows of prompt SGRBs.

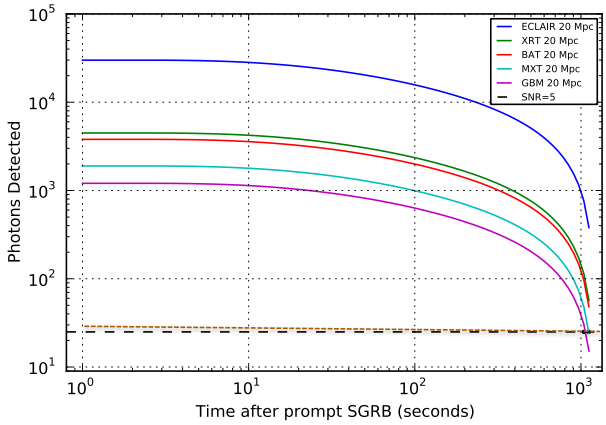

FIG. 5: Photons detected by XRT, BAT, GBM, ECLAIR, and MXT for d=20 Mpc. ECLAIR, XRT, and BAT can start their observations at 1199 seconds after the prompt SGRB, while MXT must start within 1115 seconds and GBM within 1040 seconds, as indicated by the small dots.

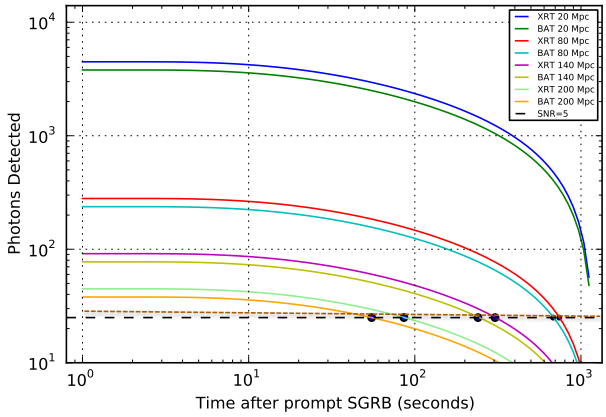

FIG. 6: Comparison of photons detected by XRT and BAT for d=20, 80, 140 and 200 Mpc. XRT / BAT must start observing within 86 s / 55s, 304 s / 240 s, 740 s / 680 s, 1199 s / 1199 for d= 200, 140, 80, and 20 Mpc respectively, after the initial prompt SGRB.

VI. CONCLUSION

Gamma-ray and/or X-ray telescopes are crucial to maximize the science return of detecting a GW signal, as ALIGO/Virgo expects to do in the coming years. The *Swift* telescope is better than the *Fermi* telescope at detecting X-ray afterglows, and thus seems to be the best current option at detecting X-ray afterglows of prompt SGRBS. the future SVOM telescope would be even more sensitive to prompt SGRB bursts and X-ray afterglows than *Swift* or *Fermi* due to ECLAIR's large effective area and sensitivity to low photon energies. Additionally, BAT onboard the *Swift* telescope may be able to detect X-ray afterglows with similar sensitivity to XRT, providing another energy range to measure the X-ray afterglows of prompt SGRBs. Verifying BAT's detection of gamma-ray bursts besides SGRB within ALIGO/Virgo's sensitivity range to NS-NS mergers may reveal more clues to BAT's full capabilities.

Acknowledgments

I graciously thank Leo Singer, Larry Price, and Stephen Privitera for mentoring during my SURF (Student Undergraduate Research Fellowship) at Caltech. Their knowledge and persistence provided for a wonderful summer in sunny California. I would also like to thank Alan Weinstein for the wonderful lectures on gravitational waves and particle physics. I also thank the California Institute of Technology, LIGO, and the National Science Foundation (NSF) for providing funding for my SURF. Additionally, I thank Van Eerten, Van Der Horst, and MacFadyen for developing the Boxfit code, and acknowledge that the development of the Boxfit code was supported in part by NASA through grant NNX10AF62G issued through the Astrophysics Theory Program and by the NSF through grant AST-1009863. Lastly, I thank my parents, brothers, and sisters for their love and support in everything I do.

[1] Abadie, J., et al. 2011a. *First Low Latency LIGO+Virgo Search for binary Inspirals and their Electromagnetic Counterparts.* arXiv:1112.6005.

[2] Abadie, J., et al. *Search for Gravitational Waves Associated With Gamma-Ray Bursts During Ligo Science Run 6 and Virgo Science Runs 2 and 4.* Paper in Preparation.

[3] Metzger, B.D., Berger, E. *What is the Most Promising Electromagnetic Counterpart of a Neutron Star Binary Merger?* The Astrophysics Journal, 746:48. 2012.

[4] Soderber et al. *The Afterglow, Energetics, and Host Galaxy of the Short-hard Gamma-ray Burst 051221a.* The Astrophysical Journal, Volum 650, p. 261 (2006).

[5] Van Eerten, H.J.and MacFadyen, Andrew. *Synthetic Off-Axis Light Curves for Low-Energy Gamma-Ray Bursts.* The Astrophysical Journal, Volume 733 (2011).

[6] Kanner, Jonah et al. *Seeking Counterparts to Advanced Ligo/Virgo Transients with Swift.* Paper in Preparation.

[7] Fairhurst, Stephen. *Triangulation of Gravitational Wave Sources with a Network of Detectors.* New Journal of Physics, 13, (2011).

[8] Abadie et al. *Predictions for the Rates of Compact Binary Coalescences Observable by Ground-based Gravitational-wave Detector.* Classical and Quantum Gravity, Volume 27, (2010).

[9] Nakar, Ehud; Gal-Yam, Avishay; Fox, Derek. *The Local Rate and the Progenitor Lifetimes of Short-hard Gamma-*

ray Bursts: Synthesis and Predictions for the Laser Interferometer Gravitational-Wave Observatory. The Astrophysical Journal, 650:281-290 (2006).

[10] Van Eerten, H.J.; Van Der Horst, A.J.; MacFadyen, Andrew. *Gamma-ray burst afterglow broadband fitting based directly on hydrodynamics simulations*. The Astrophysical Journal, Volume 749, p. 44 (2012).

[11] Gruber, D.E. *The Hard X-ray Background*. The X-ray Background, p. 52 (1992).

[12] *SWIFT* Webpage. http://www.nasa.gov/mission_pages/swift/main/index.html. 21 June 2012.

[13] C. B. Markwardt, S. D. Barthelmy, J. C. Cummings, D. Hullinger, H. A. Krimm, A. Parsons, (NASA/GSFC BAT Instrument Team). *The SWIFT BAT Software Guide*. http://swift.gsfc.nasa.gov/docs/swift/analysis/bat_swguide_v6_3.pdf. 21 June 2012.

[14] *Fermi* Gamma-Ray Space Telescope Webpage. http://gammaray.msfc.nasa.gov/gbm/. 22 June 2012.

[15] Schanne, S, et al. *The future Gamma-Ray Burst Mission SVOM*. Proceedings of Science. 28 May 2010.

[16] Götz, Diego. *SVOM: a new mission for Gamma-Ray Bursts studies*. Societa Astronomica Italiana, Volume 21, p. 162 (2012).